# Structural phase transition and soliton in an organic ferromagnetic polymer: Theoretical prediction

B. Xiong and W. Z. Wang*
*Department of Physics, Wuhan University, Wuhan 430072, People's Republic of China*
(Received 13 January 2005; revised manuscript received 5 April 2005; published 26 May 2005)

By a theoretical model consisting of Su-Schrieffer-Heeger Hamiltonian and a Hubbard term, the ground-state and soliton excitation of an organic ferromagnetic polymer *m*-polydiphenylcarbene are investigated. As the electron-phonon coupling λ increases, there is a structure phase transition from a nondegenerate symmetric phase to a twofold degenerate symmetry-breaking phase. Both of the ground-state phases are ferrimagnetic and exhibit antiferromagnetic correlation between nearest-neighboring sites. There are domain-wall solitons describing the lattice deformation and spin envelopes describing spin localization if λ is greater than a critical value, which depends on the electron-electron *U*.

DOI: 10.1103/PhysRevB.71.174431 PACS number(s): 75.10.Lp, 71.38.−k, 75.30.Fv

## I. INTRODUCTION

Molecule-based ferromagnetic compounds have attracted much attention since some organic ferrimagnets, such as p-nitrophenyl nitronyl nitroxide (p-NPNN),[1–3] Dupeyredioxyl (DTDA),[4–6] and 3-(4-chlorophenyl)-1,5-dimethyl-6-thioxoverdazyl (p-CDTV)[7] were synthesized. Recently, the discovery of ferromagnetism in polymerized fullerenes[8] stimulates renewed interest in organic ferrimagnetic systems. The search for the mechanism of ferromagnetism in organic materials is considerably challenging because these materials do not involve spins of either *d* or *f* electrons in common ferromagnetic materials.

From recent experimental studies of magnetic interactions, well-known organic magnetic molecules with the ferro(antiferro)magnetic ground state are comprised of m-phenylene-bridged organic polyradicals. On the basis of this fact, Mitani *et al.*[9] proposed a theoretical scenario to design organic high-spin polymers with the ferromagnetic ground states by linking various radicals species through an m-phenylene unit. A typical polymer model is shown in Fig. 1, in which coplanar benzene rings form a one-dimensional chain through the bridging-carbon atom. The density-function study shows that the spin densities on the bridging-carbon atoms are parallel (ferromagnetic) and antiparallel (antiferromagnetic) for the highest-spin and lowest-spin states. In fact, this polymer was studied by Iwamura *et al.*[10] as an organic ferromagnetic polymer called *m*-polydiphenylcarbene (*m*-PDPC). Its ferromagnetic properties have been clarified by the periodic Kondo-Hubbard model, in which each benzene ring has six $\pi$ electrons, while the bridging-carbon atom has a $\pi$ electron and a nonbonding localized electron.[11] The correlation between $\pi$ electrons was considered by the Hubbard model, and the ferromagnetic correlation between $\pi$ and nonbonding electrons at the bridge sites was described by the periodic Kondo model. Within mean-field theory, the ferromagnetic ground state was obtained.

However, in previous works the distortion of lattice and the electron-phonon (*e-ph*) interaction was not considered completely. It is well known that both the electron-electron (*e-e*) and electron-phonon interactions may have important effect on optical, magnetic, and electric properties of real quasi-one-dimensional materials. In polyacetylene, the *e-ph* interaction induces doubly ground-state and nonlinear excitations (solitons, polaron), which play a central role in determining the electronic properties.[12] In other conducting polymers containing phenylene rings or quinoid rings, the polaron and soliton are also investigated theoretically.[13,14] Recently, in carbon systems, the polaron and fractionally charged solitons or domains similar to the case of polyacetylene were also reported.[15–17] Motivated by these theoretical researches on hydrocarbons and carbon systems, some questions arise: are there solitons in the organic ferromagnetic system shown in Fig. 1? Is there any relation between solitons and ferromagnetism?

In this paper, we focus on the properties of the ground state and the solitons of the system in Fig. 1. The model is somewhat different from that in previous work.[11] We assume that four orbitals of bridging-carbon atoms is $sp^3$ hybridization and there are two nonbonding itinerant electrons on each bridging-carbon atom. We shall show that this assumption will not alter the qualitative spin configuration. There are eight itinerant electrons in a unit cell since each benzene ring has six $\pi$ electrons. In order to produce the ferrimagnetic ordering, the Hubbard *e-e* interaction should be considered. On the other hand, to describe the *e-ph* interaction and lattice deformation, the Su-Schrieffer-Heeger (SSH) terms[12] should

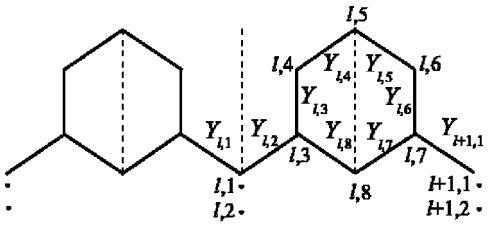


FIG. 1. Schematic structure of *m*-PDPC. The notation $l,i$ at each site labels $i$th itinerant orbitals in the $l$th unit cell. Two dots at the bridge site indicate two itinerant orbitals. $Y_{l,i}$ is the change of the $i$th bond length in the $l$th unit. Vertical dashed line labels reflection plane.

 

be included in the Hamiltonian. By using the Hartree-Fock approximation (HFA), we find that as the *e-ph* coupling increases there are two kinds of ground-state phases sequentially: a nondegenerate symmetric phase and a twofold degenerate unsymmetric phase. Because of the existence of the twofold degenerate ground state, solitons excitation can be predicted. The domain wall describing the distortion of lattice and the spin envelope describing the localization of spin coexist. Because of the competition between the *e-ph* coupling and the *e-e* interaction, the solitons exist only in a range of the *e-ph* interaction, which depends on the *e-e* interaction.

The remainder of this paper is organized as follows. The model and the computational method are given in Sec. II. The property of the ground state and the configuration of soliton are studied in Sec. III. Finally, the discussion and conclusion are given.

## II. MODEL AND COMPUTATIONAL METHOD

Based on the discussion in Sec. I, the model Hamiltonian consists of the SSH term and a Hubbard term.

$$H = H_t + H_U + H_e, \tag{1}$$

$$H_t = -\sum_{\langle li,kj\rangle,\sigma} t_{li,kj}(c^{\dagger}_{l,i,\sigma}c_{k,j,\sigma} + \text{H.c.}), \tag{2}$$

$$H_U = U\sum_{l,i} n_{l,i,\downarrow}n_{l,i,\uparrow}, \tag{3}$$

$$H_e = \frac{\kappa}{2}\sum_{l,i} Y^2_{l,i}, \tag{4}$$

where $H_t$ is the tight-binding Hamiltonian, $H_U$ is on-site Hubbard repulsion, and $H_e$ is elastic energy.

In Eqs. (2)–(4) $c^{\dagger}_{l,i,\sigma}$ ($c_{l,i,\sigma}$) are the creation (annihilation) operators of electrons with spin $\sigma=\uparrow,\downarrow$ on the $i$th orbital in the $l$th unit cell, respectively. $n_{l,i,\sigma}$ is the number operator of electrons. $\langle li,kj\rangle$ labels the nearest neighbors, $t_{li,kj}$ is the hopping integral, and $U$ is the on-site *e-e* interaction and is assumed to be common to all carbon orbitals. $\kappa$ is the elastic constant of the lattice, and $Y_{l,i}$ is the change of the $i$th bond length in the $l$th unit as shown in Fig. 1.

According to the topological structure in Fig. 1, the tight-binding Hamiltonian $H_t$ can be written explicitly

$$\begin{aligned} H_t = -\sum_{l,\sigma}\Bigg[ & \sum_{i=2}^{7}(t_0-\gamma Y_{l,i})c^{\dagger}_{l,i,\sigma}c_{l,i+1,\sigma} + (t_0-\gamma Y_{l,8})c^{\dagger}_{l,8,\sigma}c_{l,3,\sigma} \\ & + (t_0-\gamma Y_{l,2})c^{\dagger}_{l,1,\sigma}c_{l,3,\sigma} + (t_0-\gamma Y_{l,1})c^{\dagger}_{l-1,7,\sigma}(c_{l,1,\sigma}+c_{l,2,\sigma}) \\ & + \text{H.c.}\Bigg]. \end{aligned} \tag{5}$$

Here, $t_0$ is the hopping integral without distortion of lattice, and $\gamma$ is the *e-ph* coupling constant. Because the two orbitals ($l$, 1 and $l$, 2) on the bridging carbon atom are orthogonal, there is no hopping integral between them. In order to simplify the problem, the hopping integral $t_0$ is assumed to be common to all bonds.

Because the *e-e* interaction $U$ is not strong in hydrocarbon systems, the Hartree-Fock approximation (HFA) is a good start to study the band structure and distortion of the lattice for this complicated Hamiltonian. For example, for other organic ferromagnetic polymer and light-emitting polymer, the ground state and polarons are studied within the unrestricted HFA.[14,18] For carbon nanotubes and nanographite, the phase diagrams are also investigated within the unrestricted HFA.[19,20] The *e-e* interaction in Hamiltonian (3) can be treated by HFA,

$$n_{l,i,\uparrow}n_{l,i,\downarrow} = \langle n_{l,i,\uparrow}\rangle n_{l,i,\downarrow} + \langle n_{l,i,\downarrow}\rangle n_{l,i,\uparrow} - \langle n_{l,i,\uparrow}\rangle\langle n_{l,i,\downarrow}\rangle. \tag{6}$$

The single-particle wave function of the system can be expanded in site basis functions in the Wannier representation

$$\psi_{\mu} = \sum_{l,i,\sigma} Z^{\sigma}_{\mu,l,i}c^{\dagger}_{l,i,\sigma}|0\rangle, \tag{7}$$

where $|0\rangle$ is the true electron vacuum state, $\psi_{\mu}$ denotes the $\mu$th eigenvector of the Hamiltonian, and $Z^{\sigma}_{\mu,l,i}$ is the expansion coefficient.

We numerically solve the Schrödinger equation of the system

$$-\sum_{\langle li,kj\rangle} t_{li,kj}Z^{\sigma}_{\mu,k,j} + U\langle n_{l,i,-\sigma}\rangle Z^{\sigma}_{\mu,l,i} = \epsilon^{\sigma}_{\mu}Z^{\sigma}_{\mu,l,i}, \tag{8}$$

$$\langle n_{l,i,\sigma}\rangle = \sum_{\mu}^{(occ)} Z^{\sigma *}_{\mu,l,i}Z^{\sigma}_{\mu,l,i}, \tag{9}$$

where $\langle n_{l,i,\sigma}\rangle$ is the average with respect to the ground state, ($occ$) means those states occupied by electrons, and $\epsilon^{\sigma}_{\mu}$ is the $\mu$th eigenvalue.

The lattice deformation $Y_{l,i}$ can be obtained by minimizing the total energy of the system with respect to $Y_{l,i}$. The spin density $\langle S^z_{l,i}\rangle$ can be obtained by

$$\langle S^z_{l,i}\rangle = \tfrac{1}{2}(\langle n_{l,i,\uparrow}\rangle - \langle n_{l,i,\downarrow}\rangle). \tag{10}$$

The coupled Eqs. (8) and (9) can be solved self-consistently.[14,18] The starting geometry in the iterative optimization process is usually the one with any initial values of displacement $Y_{l,i}$ and the density $\langle n_{l,i,\sigma}\rangle$. Then, by solving Eqs. (8) and (9), the new density $\langle n_{l,i,\sigma}\rangle$ is obtained. By minimizing the total energy of the system, the new displacement $Y_{l,i}$ is also obtained. With these new $Y_{l,i}$ and $\langle n_{l,i,\sigma}\rangle$, the next iteration begins again. The stability of the optimized geometry is always tested by using another starting configuration and performing the optimization again.

In the following discussion, it is convenient to define a dimensionless lattice deformation

$$y_{l,i} = \gamma Y_{l,i}/t_0. \tag{11}$$

Hence the elastic energy in Hamiltonian (4) becomes

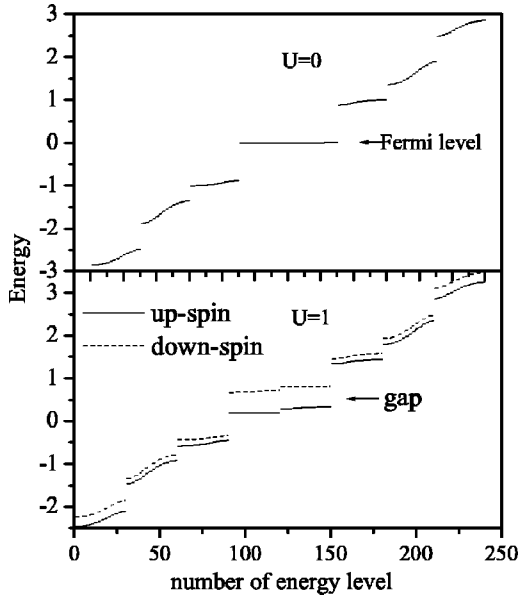


FIG. 2. Energy band structure of itinerant electrons for $U=1.0$ and 0, $\lambda=0.2$. $t_0$ is the unit of energy.

$$H_e = t_0 \sum_{l,i} y_{l,i}^2 / \pi\lambda, \tag{12}$$

where $\lambda = 2\gamma^2/(t_0\pi\kappa)$ is a dimensionless *e-ph* coupling constant.

### III. RESULTS AND DISCUSSION

We consider a periodic polymer chain that contains 30 unit cells, which have 210 carbon atoms and $N=240$ itinerant orbitals and electrons. We solve Eqs. (8) and (9) self-consistently. Because there are no reliable experimental data for the parameters in Hamiltonain (1), we take parameters similarly to the case of polyacetylene,[12,21] in which the Hubbard energy $U<4t_0$ and the *e-ph* coupling $\lambda<0.37$. In the following discussion, the hopping integral $t_0$ is chosen as the unit of energy. The band structure is shown in Fig. 2 for $U=0$ and 1.0, $\lambda=0.2$. For $U=0$, we get eight energy bands with spin degeneracy. The two localized bands with zero energy are just at the Fermi surface and are highly degenerate. In the half-filling case, just half of these two highly degenerate bands are occupied by up-spin and down-spin electrons equally. So the ground state is nonmagnetic for $U=0$. For finite $U$, the spin degeneracy of eight energy bands are removed. The electron band spectra contains eight up-spin energy bands and eight down-spin energy bands. In half-filling case, the lowest three down-spin bands and five up-spin bands are filled in the ground state. Consequently, the total spin per unit cell is $S=1$ and the ground state is ferrimagnetic.

It is well known that because of *e-ph* interaction, one-dimensional systems undergo the Peierls distortion. Figure 3 shows the distortion of lattice $y_{l,i}$ defined in Eq. (11) as a function of the *e-ph* coupling $\lambda$. It is seen that as $\lambda$ is small, the deformations $y_{l,1}=y_{l,2}$, $y_{l,4}=y_{l,5}$ are positive, while $y_{l,3}=y_{l,6}$, $y_{l,7}=y_{l,8}$ are negative. The positive and negative distortions indicate protraction and contraction of the relevant bonds, respectively. If the *e-ph* coupling is not considered, the skeleton in Fig. 1 has the point symmetry with vertical reflection plane. Apparently, for $\lambda<0.28$, the point symmetry in Fig. 1 is conserved, although with increasing $\lambda$ the distortion is enhanced. As $\lambda$ increases continuously to a critical value $\lambda_c=0.28$, the distortion is not symmetric, namely, $y_{l,1}\neq y_{l,2}$, $y_{l,4}\neq y_{l,5}$, $y_{l,3}\neq y_{l,6}$, $y_{l,7}\neq y_{l,8}$. This point symmetry is broken, although the translation symmetry with a period of seven sites is conserved. The result in Fig. 3 indicates that as $\lambda$ increases there exists a structural phase transition from the symmetric SY phase with reflection symmetry to the symmetry-breaking (SYB) phase. This behavior is quite different from that in polyacetylene, in which the Peierls distortion induces the spontaneous translation symmetry breaking, namely, dimerization.

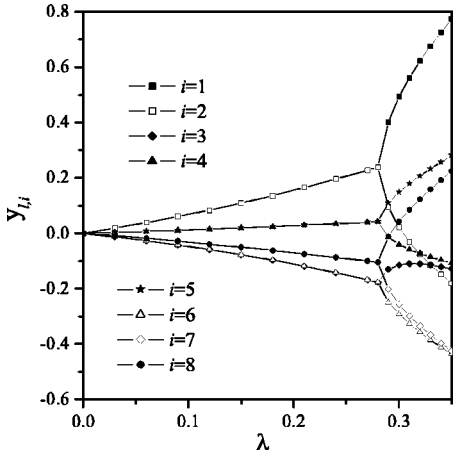


FIG. 3. Dimensionless change of bond length $y_{l,i}$ defined in Eq. (11) (also refer to Fig. 1) as a function of $\lambda$ for $U=1.0$.

The *e-e* interaction may have significant effect on the distortion. In polyacetylene, with increasing $U$, the dimerization has a maximum at a definite value of $U$.[21] However, in the present case, the feature of the distortion is quite different. Figure 4 shows the distortion $y_{l,i}$ as a function of $U$ for $\lambda=0.2$ and 0.32. It is seen that for $\lambda=0.2$, the ground state is always (SY) phase and the reflection symmetry in original lattice is kept although the distortions of different bonds are different as the *e-e* interaction $U$ increases. For $\lambda=0.32$ and $U<2.7$, the ground state is the SYB phase. As $U$ increases continuously to $U=2.7$, the reflection symmetry is recovered. Comparing Fig. 3 to Fig. 4, one can find that there exists competition between the *e-ph* coupling $\lambda$ and the *e-e* interaction $U$. The former favors the appearance of the SYB phase and the latter suppresses it. Figure 5 gives a phase diagram that shows two kinds of ground-state phases. As $U$ is small, the critical *e-ph* coupling $\lambda_c$ is nearly independent of $U$ and the appearance of SYB is mainly determined by $\lambda$. As $U>1.8$, with increasing $U$, it needs a greater $\lambda_c$ to induce the SYB phase.

Now, we discuss the spin configuration in these two kinds of ground states. Figure 6 shows the spin density $\langle S_{l,i}^z \rangle$ at eight orbitals in a unit cell. As $U$ is very small, there is no net spin at orbitals 3, 5, and 7. With increasing $U$, down-spins appear at these sites, while up-spins at orbitals 1, 2, 4, 6, and

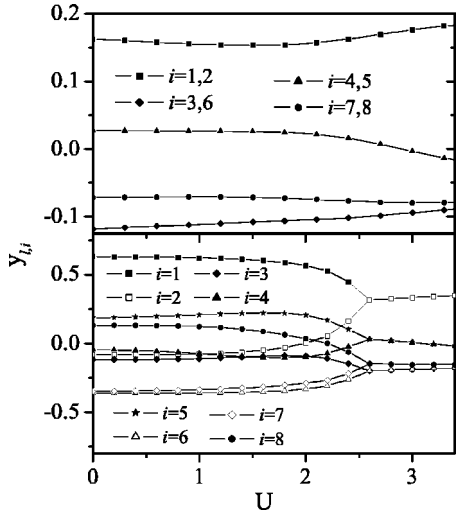


FIG. 4. $y_{l,i}$ as a function of $U$ for $\lambda=0.20$ and 0.32.

8 increase. There exist antiferromagnetic correlations between nearest neighbors, which are enhanced by the Hubbard electron-electron repulsion. Apparently, for $\lambda=0.2$, the spin densities have the symmetric property of the ground-state SY phase and their values are consistent with previous Kondo-Hubbard model.[11] For $\lambda=0.32$ and $U<2.7$, the ground state is the SYB phase. In Fig. 6(b), the spin density at orbital 4 is quite different from that at orbital 6, although they are the same in Fig. 6(a). As $U>2.7$, the spin density is redistributed with reflection symmetry.

In polyacetylene, the *e-ph* interaction induces a twofold ground state so soliton excitations exist. In the present model, as the *e-ph* coupling increases there are two kinds of ground-state phases SY and SYB, sequentially. Apparently, the symmetric (SY) phase is not degenerate so no soliton can be predicted. However, the symmetry-breaking (SYB) phase is twofold degenerate. Let us discuss it. In fact, the symmetry-breaking distortions have two distinct patterns, both of which have the same energy. One has the bonding structure as shown in Fig. 3 for $\lambda>0.28$ and is called *A* phase. If the bonding structure in *A* phase is changed by reflection operation, namely, $y_{l,1}\leftrightarrow y_{l,2}$, $y_{l,4}\leftrightarrow y_{l,5}$, $y_{l,3}\leftrightarrow y_{l,6}$,

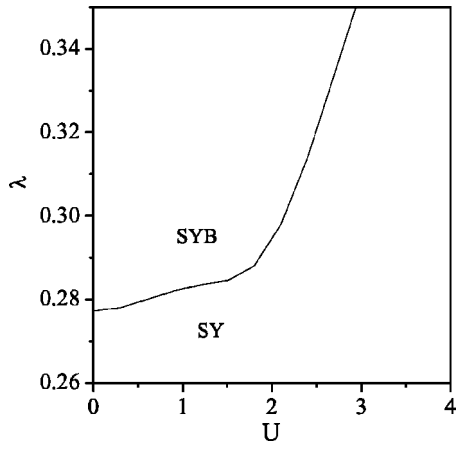


FIG. 5. Phase diagram showing two kinds of ground-state phases: symmetry (SY) and symmetry-breaking (SYB).

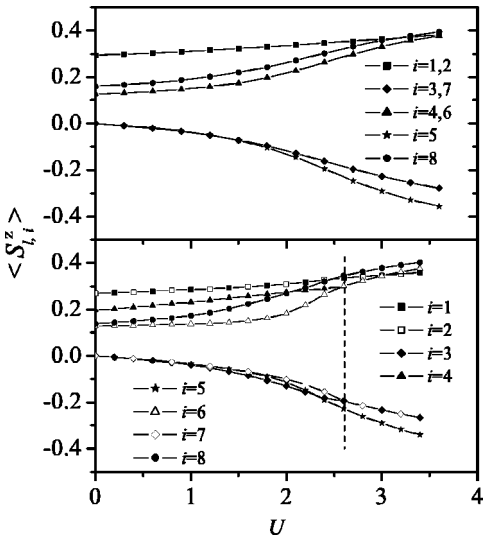


FIG. 6. Spin density $\langle S^z_{l,i}\rangle$ on eight orbitals in a unit cell as a function of $U$ for $\lambda=0.20$ and 0.32.

$y_{l,7}\leftrightarrow y_{l,8}$, then another pattern *B* phase is obtained. In this notation, $\leftrightarrow$ denotes exchanging the values of its two ends. Hence the soliton excitation can be predicted in case of the SYB state. Figure 7 shows the distortion $y_{l,i}$ when the soliton configuration appears. The domain wall in the middle of the chain has a width of about two unit cells. By the two sides of the domain wall are *A* phase and *B* phase except at the boundary of the chain, which bonding structures have the relation $y_{l,1}\leftrightarrow y_{l,2}$, $y_{l,4}\leftrightarrow y_{l,5}$, $y_{l,3}\leftrightarrow y_{l,6}$, $y_{l,7}\leftrightarrow y_{l,8}$.

The spin configurations are quite different in cases with and without a domain wall. Figure 8 shows the distribution of the spin densities along the polymer chain for eight orbitals. One can find that spin envelopes form in the middle of the chain. The spin densities by the two sides of the envelope (or in *A* phase and *B* phase) are the same for orbitals 1, 2, 5,

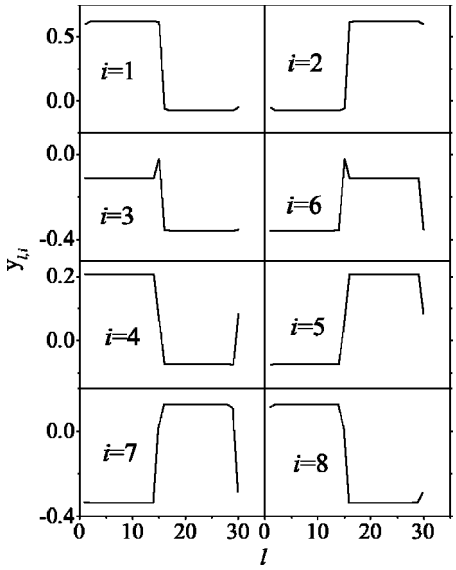


FIG. 7. $y_{l,i}$ shows the change of *i*th bond length in the *l*th unit for $U=1$ and $\lambda=0.32$. The domain wall with a width of two unit cell appears in the middle of the chain.

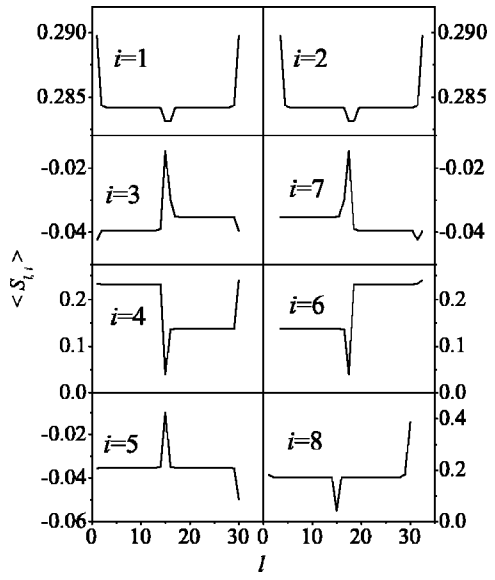


FIG. 8. Spin density $\langle S^z_{l,i}\rangle$ on the $i$th orbital in the $l$th unit for $U=1$ and $\lambda=0.32$. The spin envelopes appear in the middle of the chain.

and 8. This is nothing but the reflection symmetry of the bonding structures and spin density of *A* phase and *B* phase. Since orbitals 1, 2, 5, and 8 are on the reflection plane and not changed by the reflection operation, the spin densities at these orbitals are not changed by the reflection operation. For other orbitals 3, 4, 6, and 7, the spin densities in *A* phase and *B* phase have the relation: $\langle S^z_{l,3}\rangle \leftrightarrow \langle S^z_{l,7}\rangle$, $\langle S^z_{l,4}\rangle \leftrightarrow \langle S^z_{l,6}\rangle$. Because the twofold degenerate ground state is an essential prerequisite for the existence of solitons, the solitons exist only for $\lambda > \lambda_c$, which depends on $U$ as the ground-state SYB phase does.

It is worthy to note that the structural phase transition here is different from the previous one-dimensional (1D) Peierls transition because of the special topological structure in the present model. Let us discuss it. For $U=0$, in the 1D model, the Fermi surface is at $k=\pi/2$ for the half-filling case so that the gap appears at $k=\pi/2$ and the lattice is dimerized because of Peierls transition. If the Fermi surface is not at $k=\pi/2$ (e.g., for other filling cases or other quasi-1D lattices), the lattice does not dimerize, but probably goes to an incommensurate ground state. In the present model, for $U=0$, the two localized bands with zero energy are just at the Fermi surface and are highly degenerate. The Fermi wave vector $k_F$ is not at a definite point in Brillouin zone. As a result, if we consider *e-ph* coupling, following the picture of Peierls transition, the gap does not appear and the lattice will not dimerize or go to an incommensurate ground state because the Fermi wave vector $k_F$ cannot be determined completely. However, because of the *e-ph* coupling $\lambda$, the lattice distortion still appears by minimizing the total energy of the system. For $U=0$, we get the symmetric phase for $\lambda<\lambda_c=0.277$ and the symmetry-breaking phase for $\lambda>\lambda_c$ [refer to Fig. 5]. The behavior of the lattice distortion is similar to Fig. 3. Although the lattice distortion appears, the lattice period is still seven sites (eight orbitals). This is different from the previous 1D Peierls transition, in which the lattice period doubles the original period because the Fermi surface is at $k=\pi/2$. When the *e-e* interaction $U$ is turned on, the two localized bands at the Fermi surface split into two up-spin and two down-spin bands with very small bandwidths. The gap appears, and the ground state is ferrimagnetic. The important physics in this model is that there is a structural phase transition, which is induced by the *e-ph* coupling $\lambda$ and affected by Hubbard repulsion $U$. The gap behavior in this model is quite different from the previous 1D Hubbard-Peierls model. In present model, the gap is induced by $U$ and increased slightly by $\lambda$. Because the Fermi surface is just at the highly degenerate flat band, the *e-ph* coupling $\lambda$ cannot independently induce the gap as it does in the previous 1D Peierls transition.

In conclusion, by using a theoretical model consisting of SSH Hamiltonian and Hubbard repulsions, we have studied the ground-state and soliton excitation for an organic ferromagnetic polymer *m*-PDPC. As the *e-ph* coupling $\lambda$ increases, there are two kinds of ground-state phases, both of which are ferrimagnetic and exhibit antiferromagnetic correlation between nearest-neighboring sites. As $\lambda$ is small the ground state is a nondegenerate symmetric phase, whereas when $\lambda$ is larger than a critical value $\lambda_c$, the ground state is a twofold degenerate symmetry-breaking phase. Because of the existence of the SYB phase, there are domain-wall solitons describing the lattice deformation and spin envelopes describing spin localization. Because of the competition between the *e-ph* coupling and the *e-e* interaction, the SYB phase and solitons exist only for $\lambda>\lambda_c$, which depends on $U$. The calculated spin densities (see Fig. 6) in the present model are consistent with the previous Kondo-Hubbard model in Ref. 11, in which the estimated values of the spin densities are consistent with electron-nuclear double-resonance (ENDOR) experiments. However, the structural transition found in our model has not been reported experimentally. The calculated results could allow for the discovery of the structural transition and solitons in this system experimentally.

## ACKNOWLEDGMENTS

This work is supported by the National Science Foundation of China under the Grants No. 10004004 and No. 10374073, and FANEDD of China under Grant No. 200034.

*Email address: wzwang@whu.edu.cn

[1] M. Takahashi, P. Turek, Y. Nakazawa, M. Tamura, K. Nozawa, D. Shiomi, M. Ishikawa, and M. Kinoshita, Phys. Rev. Lett. **67**, 746 (1991).
[2] M. Kinoshita, Mol. Cryst. Liq. Cryst. Sci. Technol., Sect. A **231**, 1 (1993).
[3] M. Tamura, Y. Nakazawa, D. Shiomi, K. Kozawa, Y. Hosokoshi, M. Ishikawa, M. Takahashi, and M. Kinoshita, Chem. Phys. Lett. **186**, 401 (1991).
[4] R. Chiarelli, M. A. Novak, A. Rassat, and J. L. Tholence, Nature (London) **363**, 147 (1993).
[5] R. Chiarelli, A. Rassat, and P. Rey, J. Chem. Soc., Chem. Commun. **15**, 1081 (1992).
[6] R. Chiarelli, A. Rassat, Y. Dromzee, Y. Jeannin, M. A. Novak, and J. L. Tholence, Phys. Scr., T **49**, 706 (1993).
[7] K. Mukai, K. Nedachi, J. B. Tamali, and N. Achiwa, Chem. Phys. Lett. **214**, 559 (1993).
[8] T. L. Makarova, B. Sundqvist, R. Höhne, P. Esquinaz, Y. Kopelevich, P. Scharff, V. A. Davydov, L. S. Kashevarova, and A. R. Rakhmanina, Nature (London) **413**, 716 (2001).
[9] M. Mitani, H. Mori, Y. Takano, D. Yamaki, Y. Yoshika, and K. Yamaguchi, J. Chem. Phys. **113**, 4035 (2000).
[10] H. Iwamura, T. Sugawara, K. Itoh, and T. Takui, Mol. Cryst. Liq. Cryst. **125**, 379 (1985).
[11] K. Nasu, Phys. Rev. B **33**, 330 (1986).
[12] A. J. Heeger, S. Kivelson, J. R. Schrieffer, and W. P. Su, Rev. Mod. Phys. **60**, 781 (1988).
[13] D. S. Boudreaux, R. R. Chance, R. L. Elsenbaumer, J. E. Frommer, J. L. Bredas, and R. Silbey, Phys. Rev. B **31**, 652 (1985).
[14] K. L. Yao, S. E. Han, and L. Zhao, J. Chem. Phys. **114**, 6437 (2001).
[15] C. Chamon, Phys. Rev. B **62**, 2806 (2000).
[16] B. Hartmann and W. J. Zakrzewski, Phys. Rev. B **68**, 184302 (2003).
[17] M. Verissimo-Alves, R. B. Capaz, B. Koiller, E. Artacho, and H. Chacham, Phys. Rev. Lett. **86**, 3372 (2001).
[18] W. Z. Wang, Z. L. Liu, and K. L. Yao, Phys. Rev. B **55**, 12989 (1997).
[19] M. P. Lopez Sancho, M. C. Munoz, and L. Chico, Phys. Rev. B **63**, 165419 (2001).
[20] A. Yamashiro, Y. Shimoi, K. Harigaya, and K. Wakabayashi, Phys. Rev. B **68**, 193410 (2003).
[21] D. Baeriswyl and K. Maki, Phys. Rev. B **31**, 6633 (1985).